Electronic Supplementary Information

From LCST to Crystals: Structural Modulation of Ionic Liquids Drives Phase Transition of Poly(2-isopropyl-2-oxazoline)

Mai Kamiyama-Ueda[a),b)]‡, Takeshi Ueki[a)b)]‡, Yuji Kamiyama[a)], Ryota Tamate[a)], Keisuke Watanabe[c)], Yukiteru Katsumoto[c)]**

a) Research Center for Macromolecules and Biomaterials, National Institute of Materials and Science, 1-1 Namiki, Tsukuba, Ibaraki 305-0044 Japan
b) Graduate School of Life Science, Hokkaido University, Kita 10, Nishi 8, Kita-ku, Sapporo, Hokkaido 060-0810 Japan
c) Department of Chemistry, Faculty of Science, Fukuoka University, 8-19-1 Nanakuma, Johnan-ku, Fukuoka 814-0180, Japan

‡ M. K.-U. and T. U. contributed equally.

To whom correspondence should be addressed: UEKI.Takeshi@nims.go.jp (T.U.) and katsumoto@fukuoka-u.ac.jp (Y.K.)

Synthesis

Synthesis of Monomer[1]

2-isopropyl-2-oxazoline (iPrOx)

The reaction of iPrOx synthesis is shown in **Scheme S1**. In a three-neck flask, 23.0 g (0.33 mol) of isobutyronitrile, 43.6 g (0.71 mol) of 2-aminoethanol and 0.30 g (1.6 mmol) of zinc acetate as a catalyst were performed freeze-pump-thaw three times. Then, they were stirred and heated to 130 °C under N_2 atmosphere while refluxing. After 24 h, the raw product was dehydrated by calcium hydrate (CaH_2) overnight and purified by vacuum distillation.

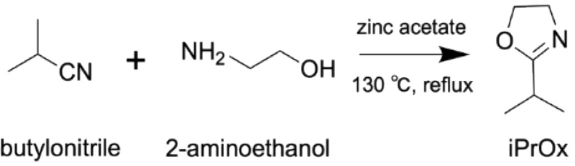

Scheme S1. Synthesis of 2-isopropyl-2-oxazoline, iPrOx monomer.

Polymerization[1]

Cationic ring-opening polymerization: Poly(2-isopropyl-2-oxazoline), PiPrOx

The synthesis of PiPrOx by cationic ring-opening polymerization is illustrated in **Scheme S2**. 1 g (8 mmol) of iPrOx as the monomer 14.9 mg (0.08 mmol) of methyl *p*-tosylate as the initiator and 15 mL distilled of acetonitrile as the solvent were heated to 80 °C. When the conversion rate reached 80%, the reaction was stopped with 1 mol/L NaOH and H_2O/methanol solution. The product was purified by dialysis 2-propanol and methanol for 3 days and against water for 2 days (Cellu-Sep H1/Membrane Filtration Products, molecular weight cut off: 1000). A white powder was obtained by freeze-drying overnight. The molecular weight (M_n) and polydispersity index (M_w/M_n) of the polymer were determined by GPC using a 10 mM LiBr/*N*, *N*-dimethylformamide (DMF) solution as the eluent.

The GPC columns (Showa Denko, Japan) were calibrated using Poly(methyl methacrylate) (PMMA) standards. (**Figure S1**, M_n = 7700 g mol^{-1}, M_w/M_n = 1.30)

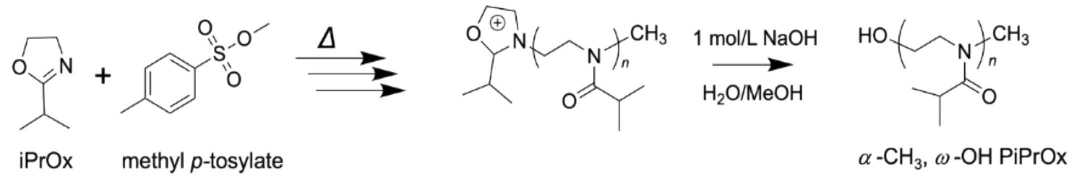

Scheme S2. Preparation of poly(2-isopropyl-2-oxazoline), PiPrOx.

Free radical polymerization: Poly(N-isopropylacrylamide), PNiPAm

Poly(*N*-isopropylacrylamide) (PNiPAm) was prepared by conventional free radical polymerization. [2] Firstly, *N*-isopropylacrylamide (NiPAm) was purified by recrystallization with *n*-hexane. 0.91 g (8 mmol) of NiPAm as the monomer, 13.3 mg (0.08 mmol) of 2,2′-azobis(isobutylonitrile) as the initiator and 4 mL toluene as the solvent were heated to 80 °C under N_2 atmosphere for 24 h. The product was recovered by reprecipitation using toluene as a good solvent and *n*-hexane as a poor solvent. The molecular weight (M_n) and polydispersity index (M_w/M_n) of the polymer were determined by GPC using a 10 mM LiBr/DMF solution as the eluent. The GPC columns (Showa Denko, Japan) were calibrated using PMMA standards. (**Figure S1**. M_n= 89000 g mol^{-1} M_w/M_n= 3.30)

Ionic liquids

Among the ILs used in this study, 1-ethyl-3-methylimidazolium trifluoromethylsulfonylimide ([C_2mim][TFSI]) was synthesized and characterized according to the procedure reported earlier[3]. All other ILs, including both [TFSI] and [BF_4]-based system, were purchased from Kanto Chemical. Prior to use, the ILs were vacuum-dried at 60 °C for over 24 hours to minimize moisture and eliminate residual volatile impurities. Consistency in phase transition behavior across multiple batches confirmed the reproducibility of the system.

Solubility screening

To identify suitable ionic liquids (ILs) for studying the phase behavior of PiPrOx and PNiPAm, we conducted a comprehensive solubility screening using 43 different ILs. Among these, ILs containing trifluoromethylsulfonylimide ([TFSI]) and tetrafluoroborate ([BF_4]) anions, combined with various alkyl imidazolium cations, were selected for detailed investigation based on the following considerations. First, [TFSI] and [BF_4] are among the most widely studied and commercially available anions in the field of ILs, making them representative choices for exploring IL-polymer interactions.[4,5] Second, [TFSI]-based ILs exhibited hydrophobicity across all tested cation combinations, ensuring compatibility with the hydrophobic polymers used in this study. Third, [BF_4]-based ILs with cations containing alkyl chains of butyl ([C_4mim]) or longer were hydrophobic and experimentally convenient to handle, particularly in terms of phase behavior measurements. These characteristics of [TFSI] and [BF_4] systems allowed for a robust and systematic investigation of polymer phase transitions in ILs, with the additional advantage of relevance to broader applications due to their widespread use and established properties. **Table S1** shows the summary of screening for PNiPAm or for PiPrOx solutions with various types of ILs. Cation and anion structure covers alkyl phosphonium ([$P_{222(C1O)}^+$], [$P_{222(C2O)}^+$], [P_{2225}^+], [P_{2228}^+], [P_{8888}^+], [P_{66614}^+]), *N*-butyl-*N*-methylpyrrolidinium ([N_{14}Pyrro$^+$]), *N*-butyl-*N*-methylpiperidinium ([N_{14}PiPe$^+$]), diethylmethylammonium ([DEMA$^+$]), *N*,*N*-diethyl-*N*-methyl-*N*-(2-methoxyethyl)ammonium ([DEME$^+$]), dicyanamide ([DCA$^-$]), chloride ([Cl$^-$]), bromide ([Br$^-$]), thiocyanate ([TCN$^-$]), octylsulfate ([C_8sulfate$^-$]), acetate, hydrogen sulfate ([HSO_4^-]), trifluoroacetate ([CF_3COO^-]), triflate ([TfO$^-$]), pentafluoroethylsulfonylimide ([BETI$^-$]), nonafluorobutylsulfonylimide ([NFSI$^-$]) and *N*,*N*-hexafluoropropane-1,3-sulfonylimide ([cTFSI$^-$]).

Turbidimetry measurements

Temperature dependence of transmittance of 633 nm light was monitored using USB2000 spectrometer (Ocean Optics, U.S.A.). The temperature is controlled by a homemade thermostat. Transmittance measurements were performed for the solution exhibiting LCST-type separation with the solution of PiPrOx. The compositions of [C_4mim][BF_4] in [C_6mim][BF_4]/[C_4mim][BF_4] IL blend are ranging from 0 mol% to 80 mol%.

FT-IR measurements

FT-IR measurements were used to characterize the conformation of PiPrOx in the PiPrOx / [C_6mim][BF_4] solution and PiPrOx/[C_2mim][TFSI] solution (IRSpirit, Shimadzu, Japan). The attenuated total reflection (ATR) technique was utilized to acquire the IR spectra of polymer solutions (20 wt%). Data processing including background subtraction of the solvent spectrum was performed using custom software (Spina)[1]. The pretreatment procedure for ATR-IR spectra, which involves subtracting the solvent spectrum from the sample spectrum has been described in previous publication[6]. IR spectra of PiPrOx/[C_6mim][BF_4] solution before and after phase separation were compared. Marker bands were found by using Density Functional Theory (DFT) calculations of the PiPrOx dimer model (*N*,*N*′-1,2-ethanediylbis-(*N*,2-dimethylpropanamide), (EdMPAm)). IR spectra of PiPrOx and EdMPAm are compared in **Figure S4**. IR spectra of solvated PiPrOx/[C_6mim][TFSI] and PiPrOx/[C_2mim][TFSI] are compared in **Figure S6**.

Thermodynamic aspects of phase behavior of polymers in ILs

Here, we discuss the difference in the effects of alkyl chain length on UCST- and LCST-phase separations (PSs). The variation in phase transition temperature resulting from the structural modification of the imidazolium cation, as illustrated in **Figure 4(b)** in body text, is noteworthy. When the cation structure changes from [C_4mim][BF_4] to [C_2C_4im][BF_4], the UCST-PS temperature of PNiPAm shifts by only 2°C. However, a change from [C_2C_4im][BF_4] to [C_6mim][BF_4] of PiPrOx leads to a nearly 30°C shift in the LCST-PS temperature. Although the polymer that are dissolved in ILs differ, LCST-PS exhibited a large transition temperature shift in response to changes in the IL structure. Considering that the UCST-PS is enthalpy-driven and the LCST-PS is entropy-driven, this significant shift is likely associated with liquid structuring effects related to entropy. It is widely accepted that ILs with longer alkyl chains (typically four or more carbons) form nanostructures consisting of polar and non-polar domains. This nano-structuring becomes more pronounced as the alkyl chain length increases. While the precise reason remains still unclear, the nano-structuring in [C_2C_4im][BF_4] is likely less developed compared to [C_6mim][BF_4], despite both cations containing the comparable total number of alkyl carbons[7-9]. This difference in the degree of nano-structuring may affect the mixing entropy of the system, leading to the substantial difference in the LCST-PS temperature observed between these ILs. This LCST-type phase behavior of [C_6mim][BF_4] compared to shorter and longer alkyl chain ILs may be partially attributed to its unique thermodynamic properties. Prior studies have suggested that [$C_n$mim][BF_4] ILs with intermediate alkyl chain lengths ($n \approx 6$) exhibit a relatively amorphous (more disordered) liquid state compared to other series of [$C_n$mim]-based ILs, characterized by the absence of a melting point and a potentially higher configurational entropy[10,11]. This less-structured state of [C_6mim][BF_4] within a series of [$C_n$mim][BF_4] might facilitate greater entropy reduction upon mixing with PiPrOx, aligning with the thermodynamic conditions required for LCST-PS. While this hypothesis provides a plausible explanation, further investigation into the nanostructuring and entropic contributions of these ILs is needed to substantiate this mechanism.

It is interesting that PNiPAm/IL systems show only the UCST-PS which is contrast to PiPrOx/IL systems. This possibly arises from the hydrogen bonding accepting/donating ability of the PNiPAm side chain, which consist of the secondary amide. The hydrogen bonding makes PNiPAm difficult to dissolve in any IL at a lower temperature. If the hydrogen bonding among the polymers breaks, IL can solvate the polymer. It has been reported that the proton of second position within the imidazolium cation ring can be hydrogen bonding donating ability[12-14]. This may compensate for the breakage of hydrogen bonds among the amide groups at a higher temperature. Not only in PNiPAm in IL solution, this consideration has also been true for the previously reported UCST-PS of poly(acrylic acid) in [C_6mim][BF_4] [15]. On the other hand, PiPrOx is a tertiary amide and acts only as a hydrogen bonding acceptor. Because the phase behavior of PiPrOx/ILs is not only UCST-type but also LCST-type, we should consider other factors other than the hydrogen bonding between polymer and IL (**Table 1**). The LCST-PS of the polymer solution is often explained by the free volume theory. It has been known that the free volume is strongly concerned with the liquid structure of solvents[16, 17]. In this theory, the dissimilarity in free volume expansion during heating of solvated solvent and of free solvent causes LCST-PS. Specifically, when the temperature rises, the difference in free volume between the solvated solvent and free solvent increases, and the system reached the critical value of χ, causing phase separation. Based on this consideration, Patterson has proposed to divide the solubility parameter χ into the enthalpy (χ_H) and entropy (χ_S) terms[16].

$$\chi = -(U_1/RT)v^2 + (C_{p1}/2R)\tau_2 \qquad \text{(A)}$$

Here, U_1, v^2, C_{p1} and τ are the evaporation energy of solvent, the difference in cohesive energy between molecules, the heat capacity, and the free volume difference between polymer and solvent, respectively. The equation (A) is expressed to model thermodynamic parameters based on differences in free volume in polymer solutions, and specifically shows how the interaction between the polymer and solvent contributes as an enthalpic and entropic contribution. The first and second terms on the right-hand side respectively represent the contribution of enthalpy and entropy to the χ parameter. The solid lines in (1) and (2) in **Figure S2** in represent such a curve, and the resultant curve of χ is shown in (3) in **Figure S2**. This represents that the polymer is less dissolved at both lower and higher temperature ranges, while it is soluble at the middle range. In the case of the PiPrOx/[C_6mim][BF_4] or PiPrOx/[C_2C_4im][BF_4] solution, we assumed that only the LCST-type phase transition at high temperatures described in the free volume theory was seen within the observed temperature range. In contrast, for the PiPrOx/[C_2mim][TFSI] or PiPrOx/[C_4mim][TFSI] combinations, the observed phase behavior followed the free volume theory where the χ parameter decreases monotonically with increasing temperature. As a result, these systems exhibited UCST-type phase transitions, opposite to the LCST-type transitions observed in PiPrOx/[C_6mim][BF_4] and PiPrOx/[C_2C_4im][BF_4]. This behavior highlights the critical role of the solvent in determining the phase transition mechanism of PiPrOx in IL systems.

Furthermore, in the context of the lattice model in Flory–Huggins theory, the number of ways to arrange a polymer chain with a *trans*-rich zig-zag conformation is considered to be smaller than that of a chain with a more flexible *gauche*-rich conformation. This suggests that the *trans*-rich conformation not only reduces the conformational entropy but also leads to a decrease in configurational entropy, due to the limited number of spatial arrangements within the lattice.

When developing stimuli-responsive polymer in IL solution for smart soft materials, it is important to control the phase transition temperature. We successfully controlled LCST-type phase separation temperature of PiPrOx in IL by utilizing IL blend. **Figure S3** shows the shift of transmittance curve of LCST-type phase transition as the mixing ratio of

[C_6mim][BF_4]/[C_4mim][BF_4] changes. **Figure S3** shows the relationship between LCST-type phase separation temperature and composition of [C_4mim][BF_4]. The LCST-type phase transition temperature of PiPrOx in [C_6mim][BF_4]/[C_4mim][BF_4] blend linearly shift from 100°C to 47°C. Controlling phase transition temperature by IL blend has already been reported previously[13, 18-20]. Although, phase transition temperature of thermo-sensitive polymers is traditionally controlled by copolymerization of another monomer against thermo-sensitive main monomer[21], it is possible to tune phase transition temperature by a remarkably simple operation of mixing IL solvents.

Table S1. Solubility test of PiPrOx or PNiPAm/IL solution. The temperature range is from 4 °C to 120 °C. Solubility of polymer in ILs is judged by naked eyes.

	[C$_2$mim][TCN]	**[C$_4$mim][TCN]**	**[C$_2$mim][DCA]**	**[C$_6$mim][Br]**	**[C$_8$mim][Br]**
PiPrOx	**LCST**	Yes	Yes	**LCST**	Yes
PNiPAm	Yes	Yes	Yes	Yes	Yes
	[C$_8$mim][Cl]	**[C$_2$mim][C$_8$sulfate]**	**[C$_2$dmim][TFSI]**	**[C$_2$mim][acetate]**	**[C$_4$mim][acetate]**
PiPrOx	**LCST**	**LCST**	**UCST**	No	No
PNiPAm	Yes	Yes	**UCST**	No	No
	[C$_2$mim][CF$_3$COO]	**[C$_4$mim][HSO$_4$]**	**[P$_{222(C1O)}$][TFSI]**	**[P$_{222(C2O)}$][TFSI]**	**[P$_{2225}$][TFSI]**
PiPrOx	No	No	**UCST**	Yes	Yes
PNiPAm	Yes	No	**UCST**	**UCST**	**UCST**
	[P$_{2228}$][TFSI]	**[P$_{66614}$][TFSI]**	**[S$_{122}$][TFSI]**	**[P$_{8888}$][TFSI]**	**[P$_{66614}$][Br]**
PiPrOx	Yes	Yes	Yes	**UCST**	Yes
PNiPAm	**UCST**	**UCST**	No	**UCST**	Yes
	[P$_{66614}$][TFSI]	**[P$_{66614}$][cTFSI]**	**[P$_{8888}$][cTFSI]**	**[P$_{66614}$][BETI]**	**[P$_{8888}$][BETI]**
PiPrOx	Yes	**UCST**	**UCST**	**UCST**	**UCST**
PNiPAm	**UCST**	**UCST**	No	**UCST**	No
	[P$_{66614}$][NFSI]	**[N$_{14}$Pyrro][TFSI]**	**[N$_{14}$Pipe][TFSI]**	**[DEMA][TfO]**	**[DEME][BF$_4$]**
PiPrOx	**UCST**	**UCST**	**UCST**	**UCST**	No
PNiPAm	No	**UCST**	**UCST**	Yes	**UCST**

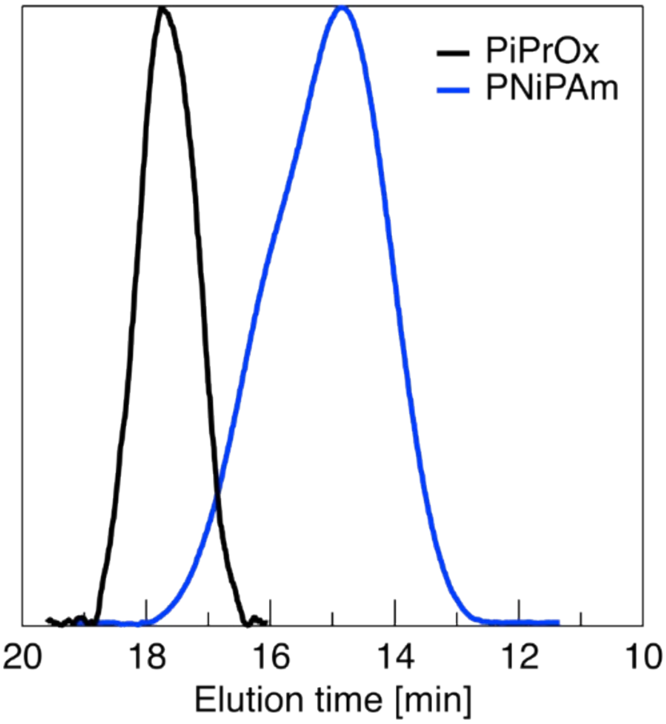

Figure S1. A GPC trace of poly(2-isopropyl-2-oxazoline) and poly(*N*-isopropylacrylamide).

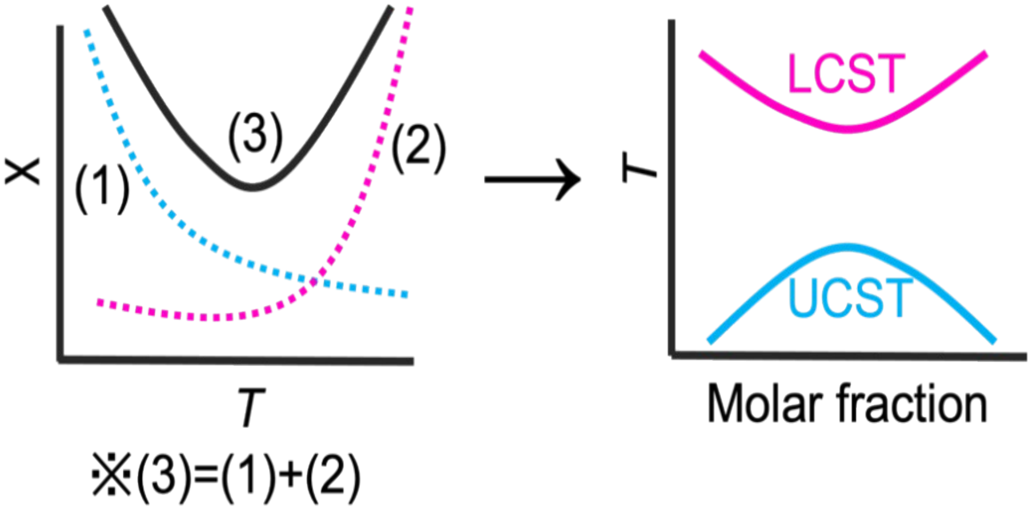

Figure S2. (Left) Schematic illustration of the χ parameter depicted by free volume theory indicated in the equation (1) of main text. The temperature dependence of the χ parameter of total: curve (3), curve (2), contribution to χ_S due to free volume dissimilarity between polymer and solvent; curve (1), contribution to χ_H due to contact energy dissimilarity between polymer and solvent. Curve (3) is obtained by the sum of (1) and (2). (Right) Phase diagram of a polymer solution showing the phase both UCST- and LCST-type.

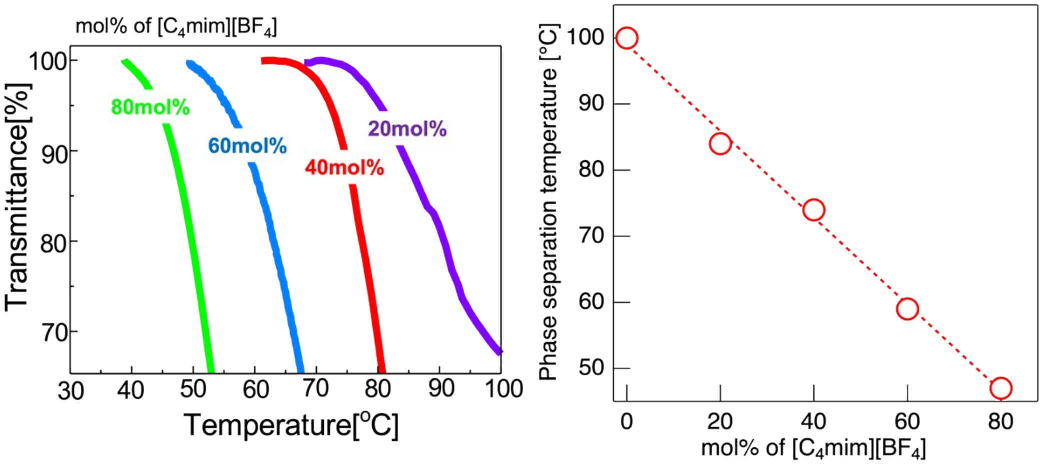

Figure S3. (a) Shift of LCST-type phase transition temperature of PiPrOx in [C_4mim][BF_4] and [C_6mim][BF_4] IL blend. (b) LCST-type phase transition temperature of PiPrOx as a function of mol% of [C_4mim][BF_4] in the ILs blend.

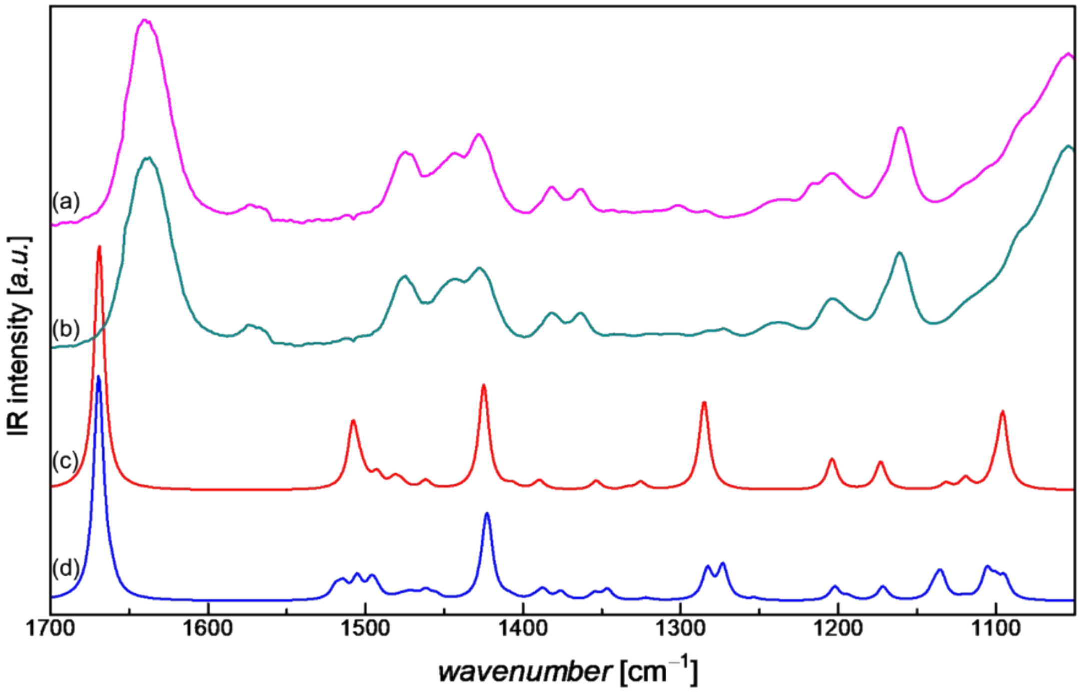

Figure S4. IR spectra of PiPrOx/[C_6mim][BF_4] solution and DFT calculated PiPrOx dimer-model, *N*,*N'*-1,2-ethanediylbis-(*N*,2-dimethylpropanamide), EdMPAm. [PiPrOx]=20 wt%. (a) phase separated in IL, (b) solvated in IL, (c) *trans* EdMPAm, (d) *gauche* EdMPAm. Chemical structure of EdMPAm is **Figure S4**(a). [1]

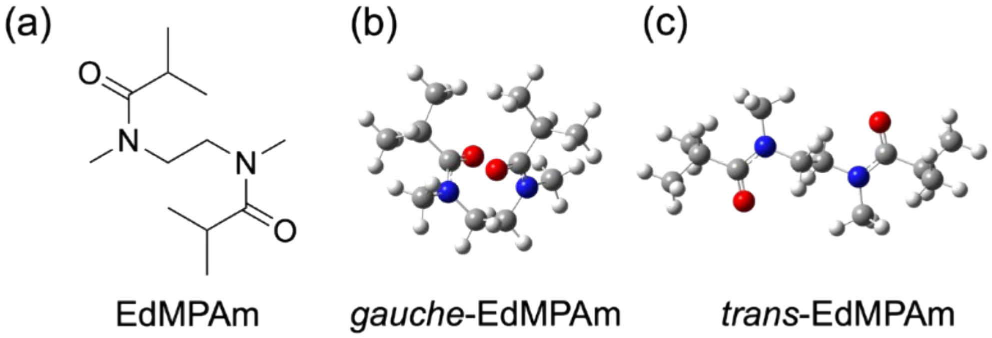

Figure S5. (a) Chemical structure of *N*, *N′*-1,2-ethanediylbis-(*N*, 2-dimethylpropanamide), EdMPAm. (b) Molecular model of *gauche*-EdMPAm and (c) *trans*-EdMPAm. [1]

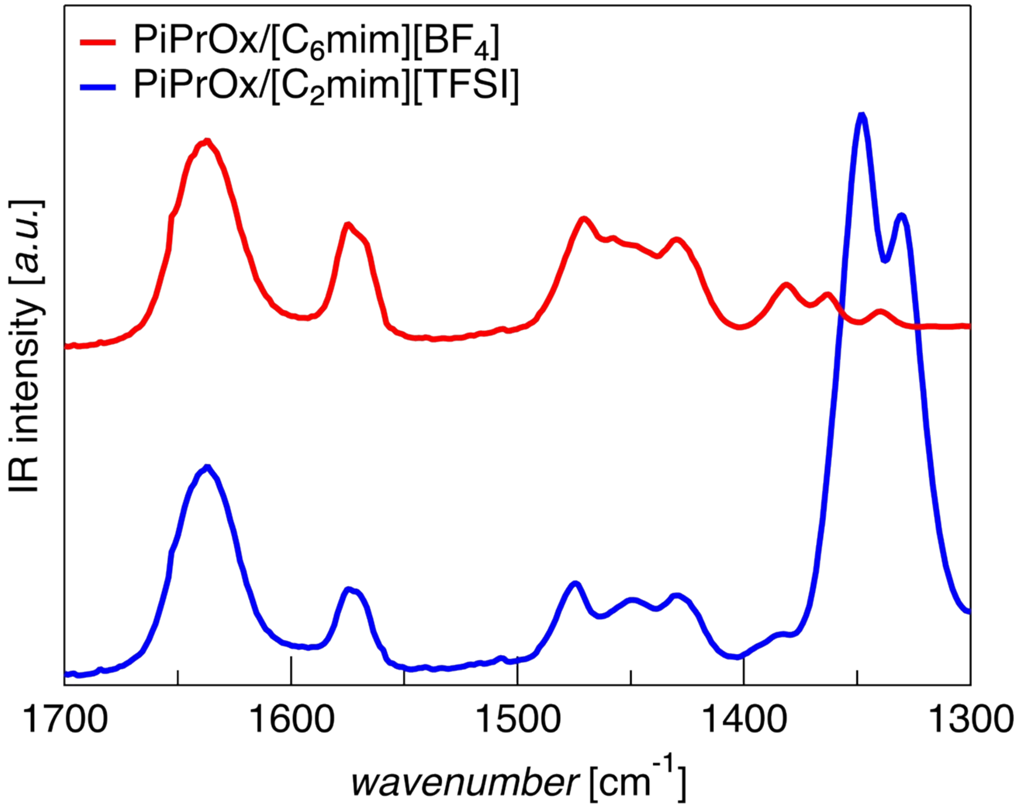

Figure S6. Before background subtraction of the solvent spectrum of IR spectra of PiPrOx/[C_6mim][BF_4] solution and PiPrOx/[C_2mim][TFSI] solution. [PiPrOx]= 20 wt%.

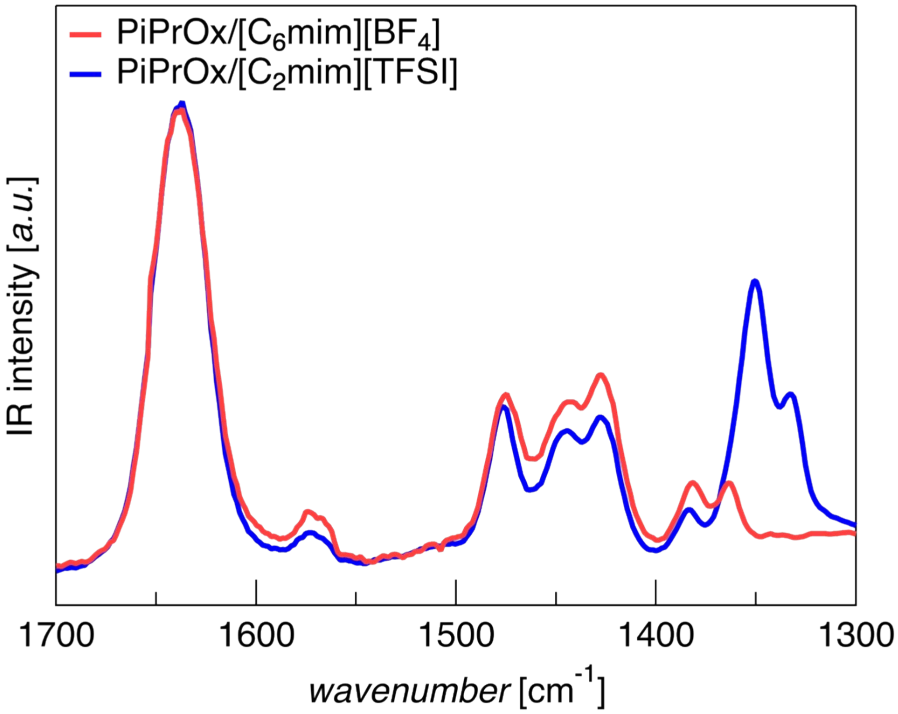

Figure S7. IR spectra of PiPrOx/[C_6mim][BF_4] solution and PiPrOx/[C_2mim][TFSI] solution. [PiPrOx]= 20 wt%

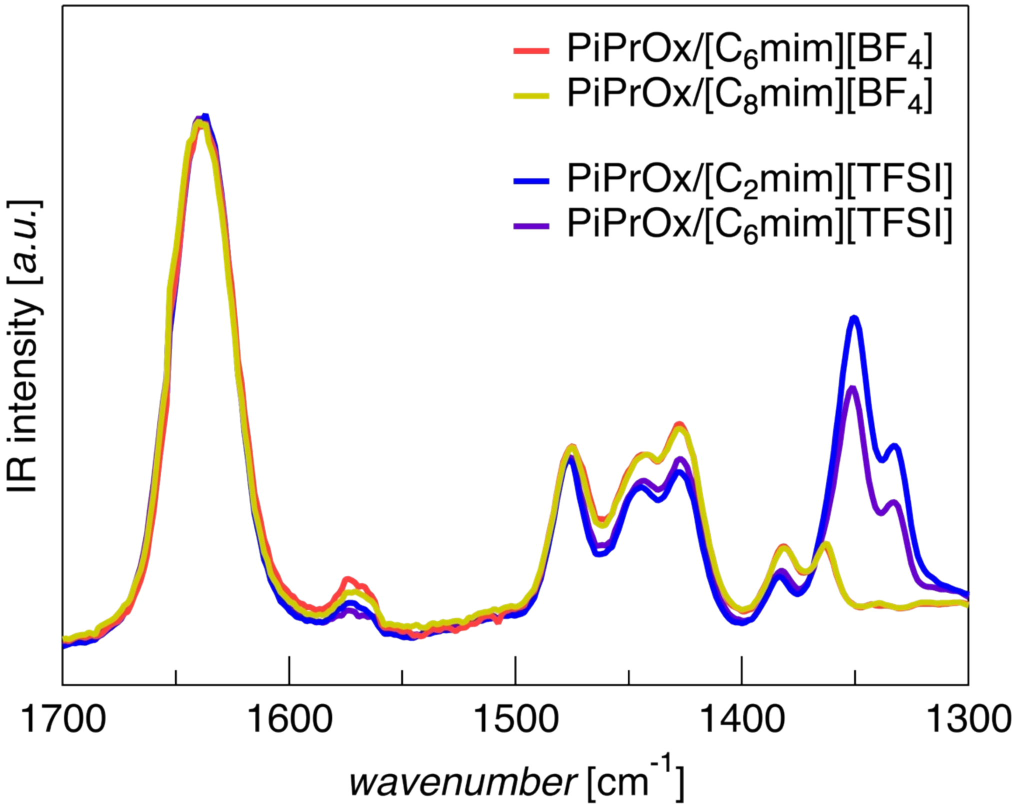

Figure S8. FT-IR spectra of PiPrOx (20 wt%) dissolved in [C_6mim][BF_4], [C_8mim][BF_4], [C_2mim][TFSI], and [C_6mim][TFSI] at room temperature. Strong C-N stretching bands at 1400-1450 cm^{-1} in [BF_4]-based ILs indicate a *trans*-rich conformation of PiPrOx. Weaker band intensities in [TFSI]-based ILs suggest that the anion structure strongly influences the conformational state of PiPrOx.

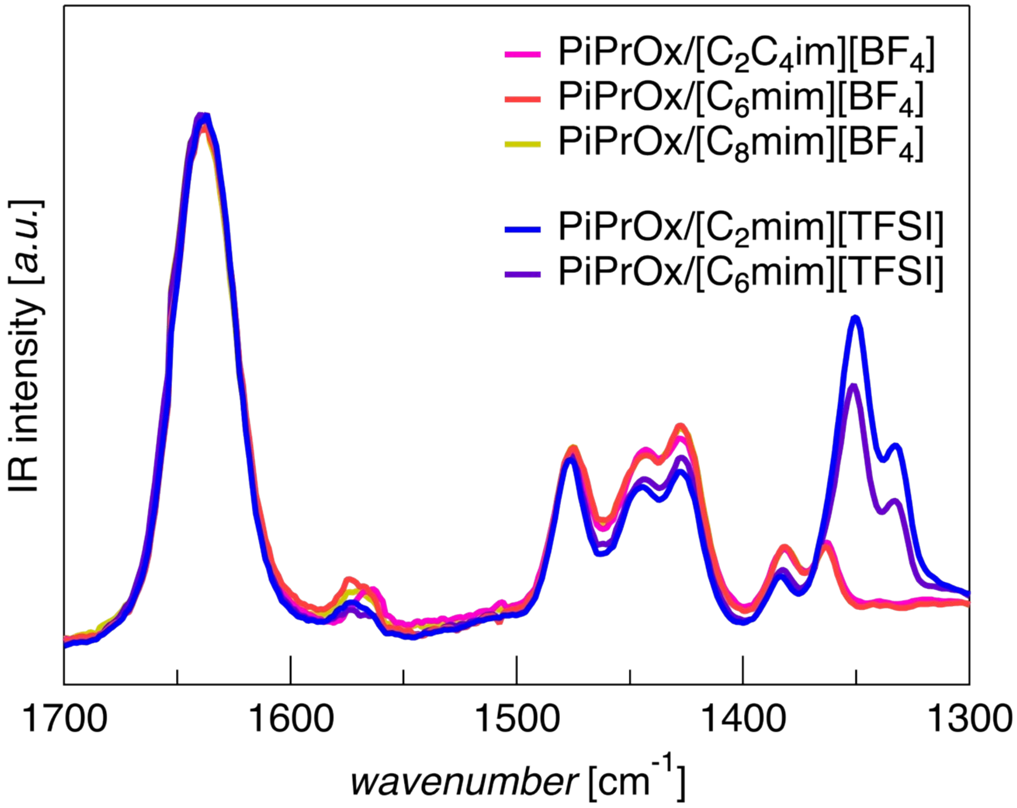

Figure S9. FT-IR spectra of PiPrOx (20 wt%) dissolved in [C$_6$mim][BF$_4$], [C$_2$C$_4$im][BF$_4$], [C$_8$mim][BF$_4$], [C$_2$mim][TFSI], and [C$_6$mim][TFSI] at room temperature. The strong C-N stretching bands observed at 1400-1450 cm^{-1} in [BF$_4$]-based samples indicate that PiPrOx adopts a *trans*-rich conformation in both ILs.

References

1. Y. Katsumoto, A. Tsuchiizu, X. Qiu and F. M. Winnik, *Macromolecules*, 2012, **45**, 3531-3541.
2. K. Homma, A. C. Chang, S. Yamamoto, T. Ueki and J. Nakanishi, *Macromol. Rapid Commun.*, 2023, **44**, 2300118.
3. H. Tokuda, S. Tsuzuki, M. A. B. H. Susan, K. Hayamizu, M. Watanabe, *J. Phys. Chem. B*, 2005, **109**, 6103-6110.
4. T. Ueki and M. Watanabe, *Bull. Chem. Soc. Jap.*, 2012, **85**, 33-50.
5. N. Winterton, *J. Mater. Chem.*, 2006, **16**, 4281.
6. Y. Katsumoto, T. Tanaka, H. Sato and Y. Ozaki, *J. Phys. Chem. A*, 2002, **106**, 3429-3435.
7. J. N. A. C. Lopes and A. A. H. Pádua, *J. Phys. Chem. B*, 2006, **110**, 3330-3335.
8. K. Dong, X. Liu, H. Dong, X. Zhang and S. Zhang, *Chem. Rev.*, 2017, **117**, 6636-6695.
9. Y. L. Wang, B. Li, S. Sarman, F. Mocci, Z. Y. Lu, J. Yuan, A. Laaksonen and M. D. Fayer, *Chem Rev*, 2020, **120**, 5798-5877.
10. J. D. Holbrey and K. R. Seddon, *Journal of the Chemical Society, Dalton Transactions*, 1999, 2133-2139.
11. K. Watanabe and T. Komai, *Bulletin of the Chemical Society of Japan*, 2021, **94**, 508-512.
12. K. Ueno, H. Tokuda and M. Watanabe, *Physical chemistry chemical physics : Physical Chemisty Chemical Physics*, 2010, **12**, 1649-1658.
13. K. Kodama, R. Tsuda, K. Niitsuma, T. Tamura, T. Ueki, H. Kokubo and M. Watanabe, *Polym. J.*, 2011, **43**, 242-248.
14. P. K. Nayak, A. P. Hathorne and H. Bermudez, *Phys. Chem. Chem. Phys.*, 2013, **15**, 1806-1809.
15. A. Kumar, P. M. Reddy and P. Venkatesu, *RSC Advances*, 2012, **2**, 6939.
16. D. Patterson, *Macromolecules*, 1969, **2**, 672-677.
17. K. S. Slow, G. Delmas and D. Patterson, *Macromolecules*, 1972, **5**, 29-34.
18. H. N. Lee and T. P. Lodge, *J. Phys. Chem. Lett.*, 2010, **1**, 1962-1966.
19. H. N. Lee and T. P. Lodge, *J. Phys. Chem. B*, 2011, **115**, 1971-1977.
20. K. Kodama, H. Nanashima, T. Ueki, H. Kokubo and M. Watanabe, *Langmuir*, 2009, **25**, 3820-3824.
21. Y. G. Takei, T. Aoki, K. Sanui, N. Ogata, T. Okano and Y. Sakurai, *Bioconjugate Chem.*, 1993, **4**, 341-346.